


Cite this: *RSC Adv.*, 2021, **11**, 38040

# Synthesis of asymmetric [bis(imidazolyl)-BH<sub>2</sub>]<sup>+</sup>-cation-based ionic liquids as potential rocket fuels†

Xue Li,<sup>a</sup> Yin Zhang,<sup>a</sup> Hongping Li,<sup>b</sup> Jing Ding,<sup>a</sup> Hui Wan<sup>\*a</sup> and Guofeng Guan<sup>\*a</sup>

As potential hypergolic fuels, hypergolic ionic liquids have attracted much attention since their development. Herein, a series of hypergolic ionic liquids based on asymmetric [bis(imidazolyl)-BH<sub>2</sub>]<sup>+</sup> cations were synthesized. The asymmetric structure of these hypergolic ionic liquids was further confirmed by NMR, infrared (IR), and high-resolution mass spectrometry-electron spray ionization (HRMS-ESI). Moreover, these hypergolic ionic liquids possess a high density of over 1.00 g cm<sup>-3</sup>, a comprehensive liquid range from -60 °C to 20 °C, and a density-specific impulse performance ranging from 305.4 to 357.8 s g cm<sup>-3</sup>, which is superior to that of unsymmetrical dimethylhydrazine. Remarkably, (1-allyl-1*H*-imidazol-3-ium-1-yl)(1-methyl-1*H*-imidazol-3-ium-1-yl) dihydroboronium dicyandiamide had the best ignition-delay time (18 ms), a high density (1.114 g cm<sup>-3</sup>), and a high value for heat of formation (400 kJ mol<sup>-1</sup>/1.48 kJ g<sup>-1</sup>). This work provides the possibility of a promising and green hypergolic fuel as rocket propellant.

Received 24th September 2021

Accepted 9th November 2021

DOI: 10.1039/d1ra07149a

rsc.li/rsc-advances

## 1. Introduction

Hydrazine and hydrazine derivatives have played a crucial role in liquid bipropellants due to their low price, low viscosity, and short ignition-delay times. However, their disadvantages, such as operating risk, expensive handling procedures, and highly carcinogenic properties, have hindered the development of unsymmetrical dimethylhydrazine (UDMH) and hydrazine derivatives.<sup>1,2</sup> Thus, researchers have attempted to find green alternatives for these derivatives of hydrazine. Ionic liquids (ILs), as environmentally friendly materials, have attracted much attention owing to their ability to be rationally designed. As energetic materials, through adjusting the anions and cations, the demand for energetic ionic liquids could be effortlessly achieved. Moreover, for liquid bipropellants, the low vapor pressure and high density of the ionic liquids also renders them a suitable choice to take the place of hydrazine derivatives.

Since 2008,<sup>3-7</sup> when dicyandiamide was first applied as the anion for energetic ionic liquids, a host of investigations have been reported. It exhibited a self-ignition phenomenon when it was touched with 100% HNO<sub>3</sub> and, since then, much emphasis has focused on the reaction with white fuming nitric acid (WFNA). Borane was first introduced into hypergolic ionic

liquids by Shreeve and co-workers,<sup>8</sup> and as an additive it exhibited pretty remarkable properties, with superior, low ignition-delay (ID) times and negligible vapor pressure, almost satisfying the critical criteria for a liquid bipropellant, compared with UDMH. Meanwhile, the role played by borane in the hypergolic reaction was also revealed by density functional theory, which showed that the strong reducing B-H bond was responsible for the superior, low ignition-delay times. Thus, introduction of reducing B-H bonds in cations or anions may markedly promote the performance of hypergolic ionic liquids. Based on the above, in order to improve the enthalpy of borohydride and cyanoborohydride anions, azoles were used to react with metal borohydride or cyanoborohydride to form the corresponding anions.<sup>8-11</sup> All these hypergolic ionic liquids exhibited excellent ignition-delay times, heats of formation, and viscosity.<sup>12-17</sup> For cations, boronium-cation-based hypergolic ionic liquids were developed to improve the fuel-rich properties of the hypergolic ionic liquids. For example, [bis(imidazolyl)-BH<sub>2</sub>]<sup>+</sup> and [imidazolyl-amine-BH<sub>2</sub>]<sup>+</sup> cations possess a high enthalpy of combustion compared with imidazolyl-based hypergolic ionic liquids, making them an attractive possibility, since for the commonly used [bis(imidazolyl)-BH<sub>2</sub>]<sup>+</sup> cations the structures were often symmetrical as a result of the synthetic routes used. For hypergolic ionic liquids, asymmetrically substituted cations are of more value for their lower melting points.<sup>18</sup> However, there were few reports of asymmetrical cations based on the [bis(imidazolyl)-BH<sub>2</sub>]<sup>+</sup> cation. Thus, the synthesis of new asymmetrical boronium-cation-based ionic liquids is of much interest, to reveal the relationship between the structure and performance of hypergolic fuels.

Herein, two types of asymmetric [bis(imidazolyl)-BH<sub>2</sub>]<sup>+</sup>-cation-based ionic liquids were successfully synthesized with

<sup>a</sup>State Key Laboratory of Materials-Oriented Chemical Engineering, College of Chemical Engineering, Jiangsu National Synergetic Innovation Center for Advanced Materials, Nanjing Tech University, Nanjing 210009, P. R. China

<sup>b</sup>Institute for Energy Research of Jiangsu University, Jiangsu University, Jiangsu 212013, P. R. China

† Electronic supplementary information (ESI) available. See DOI: 10.1039/d1ra07149a



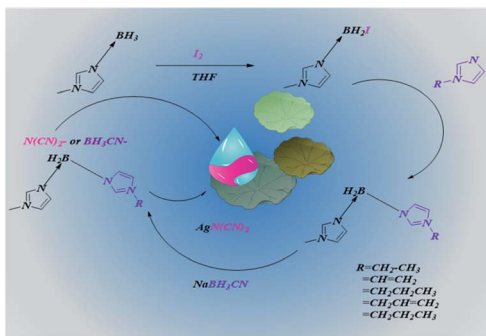


Fig. 1 The synthetic route for the asymmetric boronium-cation-based ionic liquids.

$\text{N}(\text{CN})_2^-$  and  $\text{BH}_3\text{CN}^-$  as counterions, as shown in Fig. 1. By taking advantage of the *N*-alkyl imidazole borane as the precursor, a series of asymmetric  $[\text{bis}(\text{imidazolyl})\text{-BH}_2]^+$  cations could be rationally designed through choice of the alkyl imidazole. Density, thermal stability, viscosity, and hypergolicity in touching WFNA were measured and subsequently investigated. Moreover,  $^1\text{H}$ ,  $^{13}\text{C}$ ,  $^{11}\text{B}$  NMR, and HRMS-ESI spectra were recorded to determine the asymmetric structures of the cations. To determine the heats of formation, isodesmic reactions were used. To further understand the reaction between ionic liquids and WFNA, and the differences in viscosity of these ionic liquids, the natural population charges of cations and  $\text{BH}_3\text{CN}^-$  anions were studied by non-covalent interaction (NCI) analysis using the Gaussian 09 suite of programs, and displayed using CYLview.<sup>19,20</sup> Moreover, to comprehensively evaluate the energetic properties of these ionic liquids, the heats of combustion, specific impulses, and ignition-delay times were all calculated or recorded.

## 2. Experimental section

### 2.1. Cautions

During this research no hazardous substances were used in the experiments. However, all substances should be handled carefully following safety training.

### 2.2. General methods

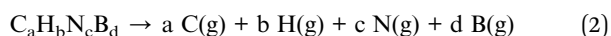
The melting point test was conducted by differential scanning calorimetry (TAQ2000, NETZSCH) at a scan rate of  $5^\circ\text{C min}^{-1}$ , while the decomposition temperature was recorded on a thermogravimetric analyzer (TGA5500, NETZSCH) with the same scan rate. HRMS-ESI spectroscopy was conducted on an Agilent 6540TOF with a Brooke solanX 70 FT-MS and Thermo QE ORBITRAP equipped with ESI.  $^1\text{H}$ ,  $^{13}\text{C}$ , and  $^{11}\text{B}$  NMR spectroscopy were performed on a Bruker Advance NEO with  $\text{DMSO-d}_6$  as the solvent. When  $^{11}\text{B}$  NMR spectra were recorded, a blank sample was run to determine the influence of the  $^{11}\text{B}$  signal arising from the borosilicate glass. Infrared spectra were obtained using tableting with potassium bromide on a Fourier-transform IR (FT-IR) spectrometer (WQF-510A). Density and viscosity measurements were recorded at  $25^\circ\text{C}$  on an Anton Parr, equipped with DMA5000M and Lovis2000ME.

### 2.3. Calculation procedure

The heat of formation is a crucial factor for the specific impulse of hypergolic ionic liquids. However, it is hard to obtain through experiments, so calculation is the best choice. Therefore, using the Gaussian 09 (Revision D.01) suite of programs, the optimization of structures, frequency analysis, and single energy points were all investigated employing B3LYP/6-311+G\*\*//MP2/6-311++G\*\*. For the boronium-cation-based ionic liquids, based on the Born-Haber cycle (shown in Scheme 1), the heat of formation (HOF) of the ionic liquid could be calculated,<sup>19,21</sup> with details as in the ESI (Tables S1 and S2).<sup>†</sup>

$$\Delta H_f(\text{salts}, 298\text{ K}) = \sum \Delta H_f^0(\text{anion}, 298\text{ K}) + \sum \Delta H_f^0(\text{cation}, 298\text{ K}) - \Delta H_L \quad (1)$$

Based on eqn (1), the HOF of the ionic liquids was obtained by calculating the value of the HOF of the anions and cations, respectively. Isodesmic reactions were further used to improve the accuracy, and details of the isodesmic reactions are shown in Scheme 2.



$$\Delta H_f(\text{g})\text{A}^{-0} = \text{EA}_A + \Delta H_f(\text{g})\text{A} \quad (3)$$

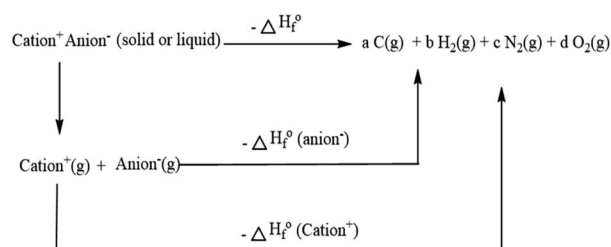
$$\Delta H_f(\text{g})\text{C}^{+0} = \text{IE}_C + \Delta H_f(\text{g})\text{C} \quad (4)$$

In addition, both  $\Delta H_f(\text{g})\text{C}^{+0}$  and  $\Delta H_f(\text{g})\text{A}^{-0}$  were achieved by calculating the HOF of the corresponding neutral molecules with an atomization reaction through eqn (2) using G2 theory, while the ionization energy ( $\text{IE}_C$ ) and electron affinity ( $\text{EA}_A$ ) were calculated using eqn (3) and (4).

$$\Delta H_L = \left[ q \left( \frac{N_X}{2} - 2 \right) + P \left( \frac{N_M}{2} - 2 \right) \right] RT + U_{\text{POT}} \quad (5)$$

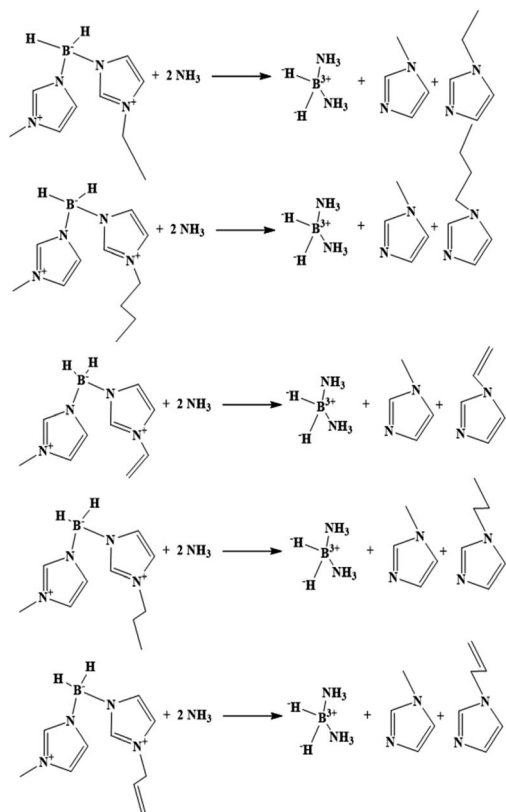
$$U_{\text{POT}} (\text{KJ mol}^{-1}) = 103.8 + 1981.2(\rho_M/M_m)^{1/3} \quad (6)$$

$\Delta H_L$  was an inherent attribute of ionic salts obtained through eqn (5) and (6).<sup>22,23</sup> For non-linear polyatomic ions,  $N_M$  and  $N_X$  possess a value of 6 on account of the  $\text{X}_{q-}$  and  $\text{M}_{p+}$  configurations. The  $U_{\text{POT}}$  (lattice potential energy) value was as shown in eqn (6), with  $\rho_M$  and  $M_m$  being the density ( $\text{g cm}^{-3}$ ) and molar mass of the ionic liquid. Based on the density and computed HOF, values of specific impulse and vacuum-specific impulse were achieved using CEA-400.



Scheme 1 Born-Haber cycle of calculation of the heat of formation for the asymmetric boronium-cation-based ionic liquids.





Scheme 2 The isodesmic reactions for the asymmetric boronium cations.

## 2.4. Synthesis of hypergolic ionic liquids

**2.4.1 Pretreatment.** 1-Methylimidazole borane complex was synthesized according to the literature with minor adjustments.<sup>24</sup> The pure 1-methylimidazole borane complex was obtained by dissolving it in dichloromethane, filtering, and removing solvent under reduced pressure. Silver dicyandiamide was prepared based on the previously reported methods.<sup>25</sup> Sodium cyanoborohydride was purchased from commercial sources. All solvents in the experiment were pretreated before use.

**2.4.2 Synthesis of compounds 2a–2e.** The synthesis procedures for compounds 2a–2e were similar to those reported in the literature, with modification.<sup>26</sup> The synthesized 1-methylimidazole borane complex (9.59 g, 100 mmol) dissolved in tetrahydrofuran (THF 100 mL) was kept at  $-30\text{ }^{\circ}\text{C}$  with stirring in a round-bottomed flask (250 mL). Then,  $\text{I}_2$  (12.69 g, 50 mmol) dissolved in THF (50 mL) was added dropwise. Most importantly, the amount of  $\text{I}_2$  added should not be in excess, which might lead to formation of the symmetric boronium-cation-based ionic liquid. The gas evolved quickly with addition of  $\text{I}_2$ , so it should be handled carefully. After complete addition, the mixture was kept for one hour with vigorous stirring, then the *N*-alkyl imidazole (100 mmol) was added to the mixture drop by drop. After that, the solution was stirred at  $25\text{ }^{\circ}\text{C}$  for one hour and refluxed overnight. During the procedure the solution became transparent and two liquid layers formed. The upper layer was THF and the bottom layer was the desired crude product. For further purification, water (150 mL) was added

with vigorous stirring to dissolve the crude product. Meanwhile, the clear solution was washed with ethyl acetate ( $3 \times 100\text{ mL}$ ), and dichloromethane was added subsequently to extract the desired product from the emulsion. Finally, a viscous liquid was obtained by removing dichloromethane. The details for compounds (2a–2e) can be found in the ESI†

**2.4.3 Synthesis of compounds 3a–3e.** An aqueous solution of the appropriate compound 2a, 2b, 2c, 2d, or 2e (20 mmol) in 40 mL  $\text{H}_2\text{O}$  was added dropwise into a suspension of silver dicyanamide (24 mmol) in 60 mL  $\text{H}_2\text{O}$ . In the absence of light, the mixture was vigorously stirred for 24 h. After filtration, water was removed by rotary evaporation to obtain a viscous and transparent liquid. The characterization of compounds 3a–3e can be found in the ESI†

**2.4.4 Synthesis of compounds 4a–4e.** An aqueous solution of the appropriate compound 2a, 2b, 2c, 2d, or 2e (20 mmol) in 40 mL  $\text{CH}_2\text{Cl}_2$  was added dropwise into a suspension of sodium cyanoborohydride (24 mmol) in 40 mL  $\text{CH}_2\text{Cl}_2$ . At room temperature, the mixture was stirred vigorously for 24 h. After filtration,  $\text{CH}_2\text{Cl}_2$  was removed by rotary evaporation to obtain a viscous and transparent liquid. The details of the compounds 4a–4e can also be found in the ESI†.

## 3. Results and discussion

### 3.1. Structure characterization of asymmetric [bis(imidazolyl)- $\text{BH}_2$ ] $^+$ -cation-based ionic liquids

Asymmetric structures play a crucial role in affecting the physical properties of ionic liquids. However, asymmetric structures are hard to obtain. By taking advantage of *N*-alkyl imidazole borane as the precursor, a series of asymmetric [bis(imidazolyl)- $\text{BH}_2$ ] $^+$  cations were obtained by rational design through choice of the alkyl imidazole. From the  $^1\text{H}$  NMR spectrum of compound 3e (as shown in Fig. 2), two peaks at 8.74 ppm and 8.66 ppm were observed belonging to the hydrogen in the imidazole ring of different alkyl imidazoles, which demonstrated the asymmetric structure of the cations. For compound 4e, characteristic peaks below 1 ppm could also be clearly seen, as a result of the  $\text{BH}_3\text{CN}^-$  anion. Moreover, the  $^{13}\text{C}$  NMR spectrum of compound 3e also demonstrated two peaks at 48.18 ppm and 35.33 ppm, which were assigned to the  $\text{CH}_2$  in 1-butylimidazole and  $\text{CH}_3$  in 1-methylimidazole, respectively. Using data from the  $^1\text{H}$  NMR and  $^{13}\text{C}$  NMR spectra, the asymmetric structure of these [bis(imidazolyl)- $\text{BH}_2$ ] $^+$  cations could be confirmed. Furthermore, a sharp band at approximately  $2427\text{ cm}^{-1}$  derived from the B–H bond was found in the IR spectra of compounds 2e, 3e, and 4e. Likewise, bands at approximately  $2233\text{ cm}^{-1}$  and  $2127\text{ cm}^{-1}$  in the IR spectra were assigned to the cyanide bonds and the nitrogen–carbon bonds of compound 3e after complete ion exchange, while bands at  $2327\text{ cm}^{-1}$  and  $2160\text{ cm}^{-1}$  were classified as the cyanide bonds in the cyanoborohydride anion of compound 4e.<sup>27</sup>

### 3.2. Density and viscosity of [bis(imidazolyl)- $\text{BH}_2$ ] $^+$ -cation-based ionic liquids

Density is an essential property of hypergolic fuels, where a high density is advantageous to the energy performance of the



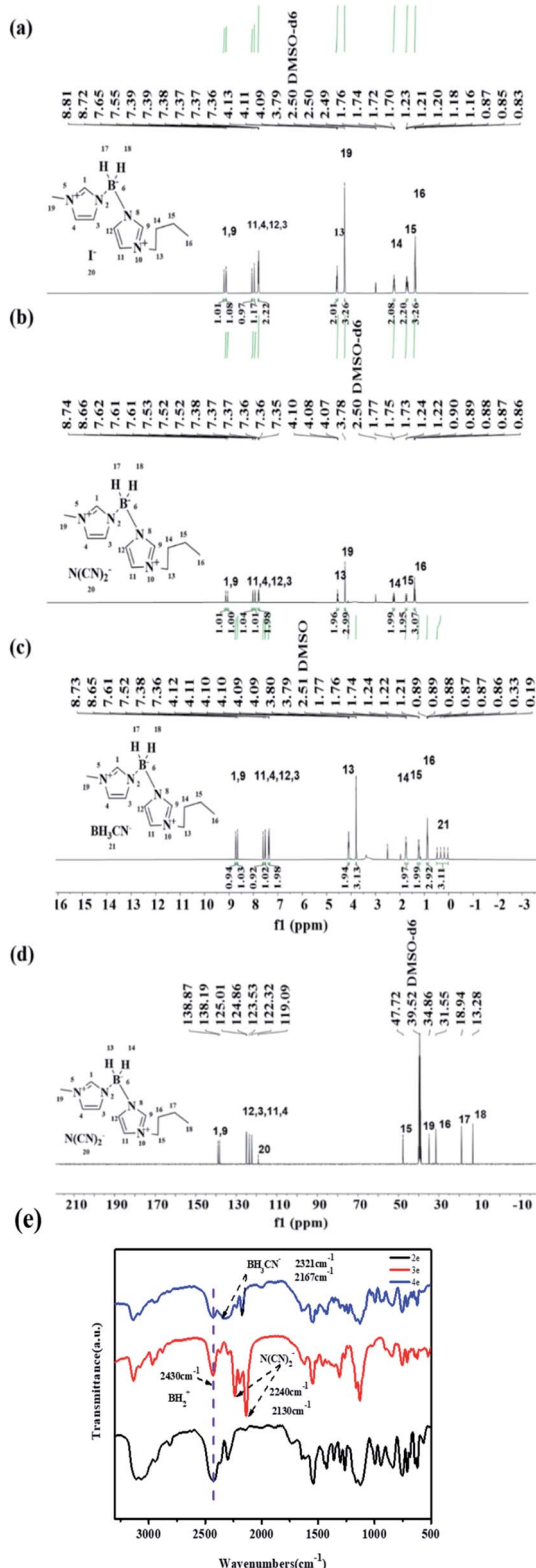


Fig. 2 (a–c)  $^1\text{H}$  NMR spectra of the compounds 2e, 3e and 4e, respectively. (d)  $^{13}\text{C}$  NMR spectrum of the compound 3e. (e) FT-IR spectra of the compounds 2e, 3e, and 4e.

hypergolic ionic liquid (HIL). In this work, each ionic liquid had a high density of nearly  $1.00 \text{ g cm}^{-3}$ , which was far higher than that of UDMH ( $0.793 \text{ g cm}^{-3}$ ). Moreover, among these

asymmetric  $[\text{bis}(\text{imidazolyl})\text{-BH}_2]^+\text{-cation-based}$  HILs, compound 3d possessed the highest density of  $1.114 \text{ g cm}^{-3}$ , and compound 4e had the lowest ( $1.003 \text{ g cm}^{-3}$ ). Obviously, for the same anions, ionic liquids with cations of similar structure show little significant difference in their density. However, for different anions, the dicyandiamide anion possessed a higher density than the cyanoborohydride anion. In addition, with regard to viscosity, slight differences in the structures of the cations lead to dramatic variations. Alongside increase in the substituent chain length of the alkyl imidazole, the viscosity was noticeably affected as a result of hydrogen bonding and van der Waals interactions of the cations,<sup>21</sup> which has an adverse effect on the mixture of fuels and oxidizer, and further impacts the ignition-delay time of the hypergolic ionic liquids. To investigate the difference in the viscosity between these asymmetric  $[\text{bis}(\text{imidazolyl})\text{-BH}_2]^+\text{-cation-based}$  ionic liquids, NCI analysis was conducted with a reduced density gradient using Multiwfn and VMD 1.9.3.<sup>28,29</sup> As shown in Fig. 3, both HILs had an evident electrostatic interaction between anions and cations. Through NCI analysis of compound A1, two spikes in the compound A1 were obtained, which can be classified as steric hindrance in the imidazole ring and the electric interaction between the anions and cations. Moreover, for the cyanoborohydride anion, there existed a large area of non-covalent interaction in B1, which, to some degree, was responsible for the higher viscosity and relatively longer ignition-delay times.

### 3.3. Thermal properties of $[\text{bis}(\text{imidazolyl})\text{-BH}_2]^+\text{-cation-based}$ ionic liquids

The melting points ( $T_m$ ) of the ionic liquids were associated with the cations that were deeply affected by the length of the

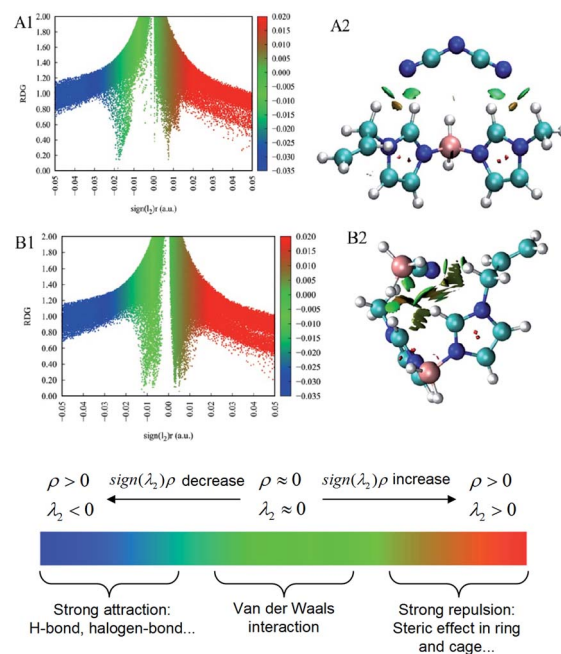


Fig. 3 NCI analysis of compounds 3d and 4d.



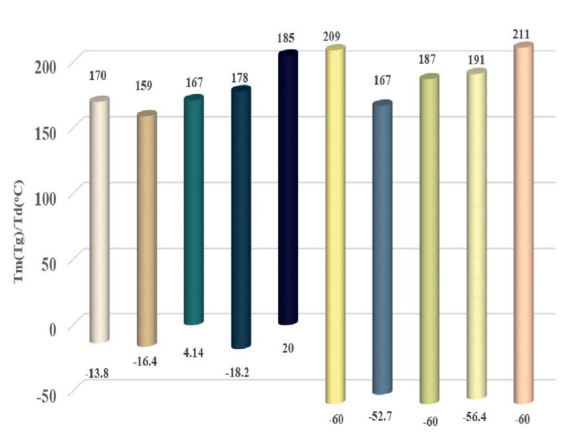


Fig. 4 Melting point or glass-transition temperature and decomposition temperature of the asymmetric boronium-cation-based hypergolic ionic liquids.

side chain of the alkyl imidazole cations. For individual [bis(imidazolyl)-BH<sub>2</sub>]<sup>+</sup>-cation-based ionic liquids, there was also an obvious increase in melting point with increase in the length of the substituents. However, compared with the bis(1-methyl-1*H*-imidazole-3-yl)dihydroboronium dicyandiamide (30 °C) reported previously,<sup>30</sup> compound **3d** had a lower melting point, although it had the highest melting point (20 °C) among the five dicyandiamide ionic liquids synthesized here. As a result, for the dicyandiamide anion, it seems that these asymmetric boronium-cation-based ionic liquids possess a lower melting point and a more comprehensive liquid range, which is beneficial for applications in a harsh environment. Furthermore, the side chain significantly impacted the decomposition temperature of the ionic liquids (as shown in Fig. 4). For these asymmetric boronium-cation-based dicyandiamides, the decomposition temperature ranged from 159 °C to 185 °C. As for the cations of compounds **3a** and **3b**, the two B–N bond lengths displayed a marked difference, which explained why compound **3b** was more unstable (Table S1†). Meanwhile, compound **3d** is more stable than compound **3c**. The heat of formation and heat of combustion (HOC) are two crucial

parameters when evaluating the performance of a bipropellant. For these hypergolic ionic liquids based on asymmetric [bis(imidazolyl)-BH<sub>2</sub>]<sup>+</sup>-cations, the values of HOC and HOF exhibited visible differences alongside differences in the degree of unsaturation and length of the side chain of the alkyl imidazole. The HOF of these asymmetric [bis(imidazolyl)-BH<sub>2</sub>]<sup>+</sup>-cation-based ionic liquids ranged from 26 kJ mol<sup>−1</sup> to 400 kJ mol<sup>−1</sup>, and most were higher than that of UDMH (51.9 kJ mol<sup>−1</sup>)<sup>27</sup>. In addition, all the HOC values for these HILs were below −7330 kJ mol<sup>−1</sup>, which is far lower than that of UDMH (−1982.6 kJ mol<sup>−1</sup>), meaning that more energy is released when the IL fuels react with an oxidizer (Fig. 5). Thus, with respect to the HOF and HOC values, there is no doubt that these asymmetric [bis(imidazolyl)-BH<sub>2</sub>]<sup>+</sup>-cation-based HILs are promising candidates as alternatives for hydrazine derivatives.

### 3.4. Ignition test with WFNA

Ignition-delay time is also an essential factor in assessing the performance of hypergolic fuels. In terms of traditional liquid-propellant rocket engines, the ignition-delay time should be shorter than 50 ms to prevent detonation and ensure the safety of the rocket engine. For these ionic liquids, about 23 mg of fuels were added into a 10 mL penicillin bottle containing 0.5 mL 100% HNO<sub>3</sub>. The process (Fig. 6) was recorded with a high-speed camera at 1000 frames per second (fps). As shown in Table 1, it could be seen that the ID time varied from 18 ms to 628 ms. Most dicyandiamide ionic liquids had an ID time below

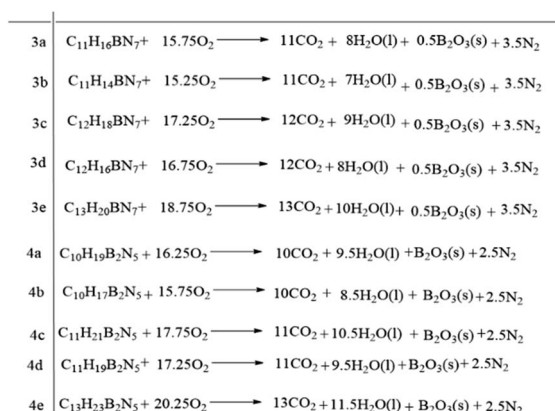


Fig. 5 Combustion reactions for asymmetric boronium-cation-based ionic liquids.

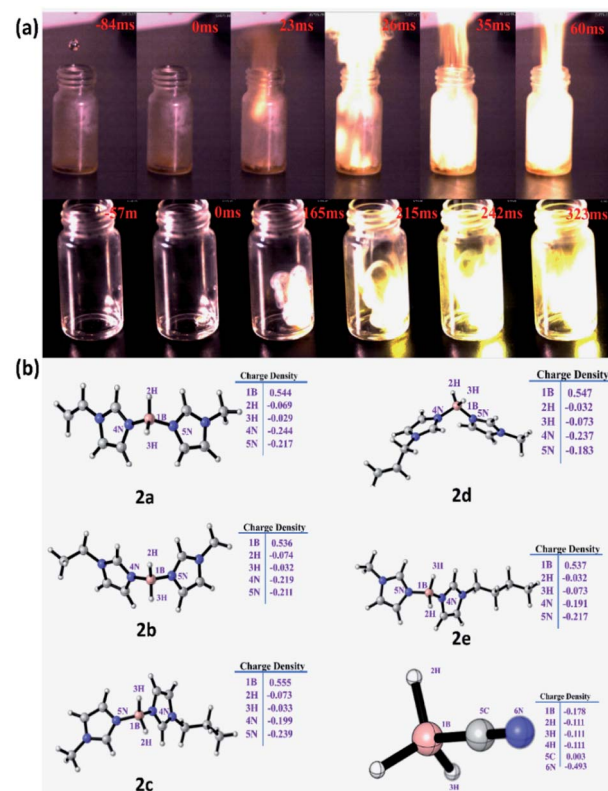


Fig. 6 (a) Test of the ID time with high-speed camera photographs at 1000 fps (**3b** and **4b** contacting WFNA). (b) NPA charges of cations for compounds **2a**–**2e** and BH<sub>3</sub>CN<sup>−</sup>, respectively.



Table 1 Physical properties and specific impulses of new ionic liquids

ILs	$\rho^a$ [g cm <sup>-3</sup> ]	$\eta^a$ [mPa s]	$\Delta H_f^b$ [kJ mol <sup>-1</sup> /kJ g <sup>-1</sup> ]	$\Delta H_c^c$ [kJ mol <sup>-1</sup> ]	ID <sup>d</sup> [ms]	Isp <sup>e</sup> [s]	$\rho$ Isp <sup>f</sup> [s g cm <sup>-3</sup> ]
3a	1.097	66	261/1.02	-7512.7	28	280.7	307.9
3b	1.091	186	373/1.46	-7338.9	21	279.9	305.4
3c	1.092	83	244/0.90	-8174.9	45	281.2	307.1
3d	1.114	93	400/1.48	-8045.1	18	280.9	312.9
3e	1.090	142	227/0.80	-8837.2	61	281.7	307.1
4a	1.061	201	54/0.23	-7977.51	166	330.2	350.3
4b	1.085	1126	163/0.67	-7637.8	200	329.8	357.8
4c	1.025	295	41/0.18	-8602.9	390	330.5	338.8
4d	1.079	356	194/0.80	-8510.7	158	330.8	357.0
4e	1.003	343	26/0.10	-9308.74	621	330.8	328.2
UDMH	0.79	0.49	51.9/0.804	-1982.6	4.8	327.2	258.5

<sup>a</sup> Density and viscosity at 25 °C. <sup>b</sup> Heat of formation. <sup>c</sup> Heat of combustion. <sup>d</sup> Ignition delay time with WFNA. <sup>e</sup> Vacuum-specific impulse and density-specific impulse: pressure 0.95 MPa; area expansion ratio of nozzle 70; oxidizer N<sub>2</sub>O<sub>4</sub> (equivalence ratio = 1.0) (CEA program). <sup>f</sup> Calculated methods derived from the literature.<sup>31</sup>

50 ms to guarantee security in their use, while the cyanoborohydride anion exhibited a worse ID time due to its poor performance with regard to viscosity. In particular, N(CN<sub>2</sub>)<sup>-</sup> anion compounds **3d** and **3a** had ignition-delay times of 18 ms and 28 ms respectively, far below 50 ms, which could be comparable with bis(1-allyl-1*H*-imidazole-3-yl)dihydroboronium dicyanamide (18 ms). Furthermore, as shown in Table 1, the ignition-delay times of these HILs showed an apparent increase with increase in the length of the side chain of the imidazole ring, and the ID time of the HIL was also profoundly affected by the unsaturated side chain of the imidazole ring, with both compounds **3b** and **3d** possessing shorter ignition-delay times than the other ionic liquids. Interestingly, the flame for the cyanoborohydride anions was brighter (Fig. 6) than those of the dicyandiamide ionic liquids, which might be a result of the high boron content in these HILs.

To investigate the difference of viscosity between dicyandiamide and cyanoborohydride anion, NCI (non-covalent interaction) analysis was conducted. Moreover, the natural population charges of cations and BH<sub>3</sub>CN<sup>-</sup> anion were further calculated to demonstrate the excellent performance in the ignition delay times. As shown in Fig. 6, the negative charge in the B-H bonds contributed to the superior performance of the ID time for these asymmetric [bis(imidazolyl)-BH<sub>2</sub>]<sup>+</sup>-cation-based ionic liquids, as displayed using CYLview 1.0. However, higher viscosity restricted the application of these cyanoborohydride HILs. The viscosity had a significant influence on the performance of the hypergolic ionic liquids mentioned above. For these ionic liquids, the cyanoborohydride anion had a higher consistency than that of the dicyandiamide anion, as shown in Table 1.

### 3.5. Specific impulse

Using the NASA-CEA program, by taking advantage of the values of the heat of formation and density, both the vacuum-specific impulse and density-specific impulse of these asymmetric [bis(imidazolyl)-BH<sub>2</sub>]<sup>+</sup>-cation-based hypergolic ionic liquids can be obtained, which are superior to those of traditional hypergolic ionic liquids and UDMH. From Table 1, most of the hypergolic ionic liquids synthesized here nearly met the requirements for use in rocket fuel. Even for compound **3b**, the density-specific impulse

was 305.4 s g cm<sup>-3</sup>, which is higher than for UDMH (258.5 s g cm<sup>-3</sup>). In particular, the BH<sub>3</sub>CN<sup>-</sup> anion had a higher boron content than the dicyandiamide anion, resulting from a higher vacuum-specific impulse, as shown in Table 1.

## 4. Conclusions

In summary, a novel type of asymmetric boronium-cation-based ionic liquid was successfully synthesized. With respect to the melting points, heats of formation, and decomposition temperatures, the unsaturated side chains of the alkyl imidazole and the asymmetric structures of the cations were shown to play a vital role in these aspects, through theoretical and experimental analysis. Moreover, all the hypergolic ionic liquids had higher heats of formation and higher densities than UDMH. Overall, the (1-allyl-1*H*-imidazol-3-ium-1-yl)(1-methyl-1*H*-imidazol-3-ium-1-yl) dihydroboronium dicyandiamide possessed the lowest ignition-delay time (18 ms) and the highest density (1.114 g cm<sup>-3</sup>), as well as the highest heat of formation, among the asymmetric ionic liquids. This means that it is a promising material for use as a propellant and these asymmetrical boronium cations can be taken into consideration for the design of new hypergolic ionic liquids.

## Conflicts of interest

There are no conflicts to declare.

## Acknowledgements

We would like to thank the National Natural Science Foundation of China (No. 21878159, No. 21706131, No. 22078159 and No. U19B2001) and the Natural Science Foundation of Jiangsu Province of China (No. BK20181378) for financial support, and the High-Performance Computing Center of Nanjing Tech University for supporting the computational resources.



## Notes and references

- 1 C. A. V. Salvador and F. S. Costa, *J. Propul. Power*, 2006, **22**, 1362–1372.
- 2 Q. Zhang and J. N. M. Shreeve, *Chem. Rev.*, 2014, **114**, 10527–10574.
- 3 S. Schneider, T. Hawkins, M. Rosander, G. Vaghjiani, S. Chambreau and G. Drake, *Energy Fuels*, 2008, **22**, 2871–2872.
- 4 T. Fei, H. Cai, Y. Zhang, L. Liu and S. Zhang, *J. Energ. Mater.*, 2016, **34**, 138–151.
- 5 R. Fareghi-Alamdari and R. Hatefipour, *J. Mol. Liq.*, 2017, **225**, 793–799.
- 6 R. Fareghi-Alamdari, F. Ghorbani-Zamani and N. Zekri, *RSC Adv.*, 2016, **6**, 26386–26391.
- 7 Y. Gao, H. Gao, C. Piekarski and J. M. Shreeve, *Eur. J. Inorg. Chem.*, 2007, **2007**, 4965–4972.
- 8 S. Li, H. Gao and J. M. Shreeve, *Angew. Chem., Int. Ed.*, 2014, **53**, 2969–2972.
- 9 P. D. McCrary, P. S. Barber, S. P. Kelley and R. D. Rogers, *Inorg. Chem.*, 2014, **53**, 4770–4776.
- 10 H. Gao and J. M. Shreeve, *J. Mater. Chem.*, 2012, **22**, 11022.
- 11 Y. Liu, D. Zhang, Y. Ma, J. Li, Y. Bai and J. Peng, *Curr. Org. Synth.*, 2019, **16**, 276–282.
- 12 X. Li, C. Wang, H. Li, F. Nie, H. Yin and F. Chen, *J. Mater. Chem. A*, 2017, **5**, 15525–15528.
- 13 N. Jiao, Y. Zhang, H. Li, L. Liu and S. Zhang, *Chem.-Asian J.*, 2018, **13**, 1932–1940.
- 14 X. Li, H. Huo, H. Li, F. Nie, H. Yin and F. Chen, *Chem. Commun.*, 2017, **53**, 8300–8303.
- 15 Z. Wang, Y. Jin, W. Zhang, B. Wang, T. Liu, J. Zhang and Q. Zhang, *Dalton Trans.*, 2019, **48**, 6198–6204.
- 16 H. Li, Y. Zhang, L. Liu, N. Jiao, X. Meng and S. Zhang, *New J. Chem.*, 2018, **42**, 3568–3573.
- 17 Z. Zhang, Z. Zhao, B. Wang and J. Zhang, *Green Energy Environ.*, 2020, **6**, 794–822.
- 18 Y. Zhang, H. Gao, Y. Joo and J. M. Shreeve, *Angew. Chem., Int. Ed.*, 2011, **50**, 9554–9562.
- 19 R. A., M. J. Frisch, G. W. Trucks, H. B. Schlegel, G. E. Scuseria, M. A. Robb, J. R. Cheeseman, G. Scalmani, V. Barone, G. A. Petersson, H. Nakatsuji, X. Li, M. Caricato, A. Marenich, J. Bloino, B. G. Janesko, R. Gomperts, B. Mennucci, H. P. Hratchian, J. V. Ortiz, A. F. Izmaylov, J. L. Sonnenberg, D. Williams-Young, F. Ding, F. Lipparini, F. Egidi, J. Goings, B. Peng, A. Petrone, T. Henderson, D. Ranasinghe, V. G. Zakrzewski, J. Gao, N. Rega, G. Zheng, W. Liang, M. Hada, M. Ehara, K. Toyota, R. Fukuda, J. Hasegawa, M. Ishida, T. Nakajima, Y. Honda, O. Kitao, H. Nakai, T. Vreven, K. Throssell, J. A. Montgomery Jr, J. E. Peralta, F. Ogliaro, M. Bearpark, J. J. Heyd, E. , K. N. Kudin, V. N. Staroverov, T. Keith, R. Kobayashi, J. Normand, K. Raghavachari, A. Rendell, J. C. Burant, S. S. Iyengar, J. Tomasi, M. Cossi, J. M. Millam, M. Klene, C. Adamo, R. Cammi, J. W. Ochterski, R. L. Martin, K. Morokuma, O. Farkas, J. B. Foresman, and D. J. Fox, *Gaussian 09*, Gaussian, Inc., Wallingford CT, 2016.
- 20 C. Y. Legault, *CYLVview, 1.0b*, Université de Sherbrooke, 2009, (<http://www.cylview.org>).
- 21 G. Tao, M. Tang, L. He, S. Ji, F. Nie and M. Huang, *Eur. J. Inorg. Chem.*, 2012, **2012**, 3070–3078.
- 22 H. D. B. Jenkins, D. Tudela and L. Glasser, *Inorg. Chem.*, 2002, **41**, 2364–2367.
- 23 H. D. B. Jenkins, H. K. Roobottom, J. Passmore and L. Glasser, *Inorg. Chem.*, 1999, **38**, 3609–3620.
- 24 S. Huang, W. Zhang, T. Liu, K. Wang, X. Qi, J. Zhang and Q. Zhang, *Chem.-Asian J.*, 2016, **11**, 3528–3533.
- 25 T. Zhang, L. Liu, C. Li, Y. Zhang, Z. Li and S. Zhang, *J. Mol. Struct.*, 2014, **1067**, 195–204.
- 26 G. Agrifoglio, *Inorg. Chim. Acta*, 1992, **197**, 159–162.
- 27 V. K. Bhosale and P. S. Kulkarni, *New J. Chem.*, 2017, **41**, 1250–1258.
- 28 T. Lu and F. Chen, *J. Comput. Chem.*, 2012, **33**, 580–592.
- 29 W. Humphrey, A. Dalke and K. Schulten, *J. Mol. Graphics*, 1996, **14**(33–38), 27–28.
- 30 K. Wang, Y. Zhang, D. Chand, D. A. Parrish and J. M. Shreeve, *Chem.-Eur. J.*, 2012, **18**, 16931–16937.
- 31 C. Sun and S. Tang, *Energy Fuels*, 2020, **34**, 15068–15071.

